

# A non-QE signature of $\nu_e$ appearance in a water Cherenkov detector

A. Asratyan and V. Verebryusov

ITEP Moscow, Russia

November 20, 2018

## Abstract

We argue that analyzing the  $\nu_e$ -induced CC reaction  $\nu_e n \rightarrow e^- \pi^0 p$  along with the quasielastic reaction  $\nu_e n \rightarrow e^- p$  may significantly enhance the sensitivity of a water Cherenkov detector to the subleading oscillation  $\nu_\mu \rightarrow \nu_e$  at neutrino energies  $\sim 2-3$  GeV, as projected for the off-axis neutrino beam of NuMI. At the level of standard selections, the multi-ring signal of  $\nu_\mu \rightarrow \nu_e$  yielded by this  $\pi^0$ -producing reaction is comparable to the 1-ring (quasielastic) signal in statistical significance. The neutral-current background to  $\nu_e n \rightarrow e^- \pi^0 p$  can be further suppressed by analyzing spatial separation between the reconstructed primary vertex and the vertices of individual rings.

Detecting the "subleading" oscillation  $\nu_\mu \rightarrow \nu_e$  in an off-axis beam with peak energy near 2-3 GeV has emerged as one of the major goals of the NuMI program [1], addressed at a Fermilab workshop in May 2002 [2] and in a recent Letter of Intent on the subject [3]. A 2.5-3 times bigger baseline than in the proposed JHF2K experiment [4], that will operate at a lower beam energy of  $E_\nu \sim 0.7-0.8$  GeV, will allow to probe the matter effect by comparing the probabilities of the

$\nu_\mu \rightarrow \nu_e$  and  $\bar{\nu}_\mu \rightarrow \bar{\nu}_e$  transitions<sup>1</sup>. Detector options discussed include a fine-grained low-density calorimeter, a liquid-Argon TPC, and a water Cherenkov spectrometer. Of these, the latter option is based on proven techniques, has an excellent record in neutrino physics [5], and offers best opportunities in terms of maximum target mass at reasonable cost. It appears however that, in the quasielastic mode only discussed thus far, a water Cherenkov detector will perform worse in NuMI than in JHF2K because of more background to 1-ring electronlike events from single- $\pi^0$  production in NC collisions [3]. It has been estimated [6] that, due to considerable NC background to quasielastics, a water Cherenkov detector needs to be  $\sim 3$  times as massive as a low-density calorimeter in order to reach similar sensitivity to  $\nu_\mu \rightarrow \nu_e$  in NuMI conditions. But can the performance of a water Cherenkov detector at  $E_\nu \sim 2\text{--}3$  GeV be boosted by going beyond quasielastics ?

We believe that at neutrino energies  $\sim 2$  GeV or higher, the sensitivity to  $\nu_\mu \rightarrow \nu_e$  can be enhanced by also detecting the CC reactions producing a  $\pi^0$ ,  $\nu_e n \rightarrow e^- \pi^0 p$  and  $\bar{\nu}_e p \rightarrow e^+ \pi^0 n$ , that largely proceed through excitation of the  $\Delta(1232)$  and other baryon resonances<sup>2</sup>. Compared to  $\nu_e n \rightarrow e^- p$  and  $\bar{\nu}_e p \rightarrow e^+ n$ , the cross sections of these reactions<sup>3</sup> are small for  $E_\nu < 1$  GeV but significant at  $E_\nu \sim 2\text{--}3$  GeV (see Fig. 1), so that these processes may be relevant to NuMI rather than JHF2K. Depending on whether or not the  $\pi^0$  has been fully reconstructed, two different signatures are possible for a water Cherenkov detector:

- Three  $e$ -like rings, of which two fit to  $\pi^0 \rightarrow \gamma\gamma$ ;
- Two  $e$ -like rings that would not fit to a  $\pi^0$ .

Despite a smaller cross section, the  $\pi^0$ -producing reaction may be competitive with

---

<sup>1</sup>Without antineutrino running, this can be done by comparing the  $\nu_\mu \rightarrow \nu_e$  probabilities for a longer (NuMI) and shorter (JHF2K) baselines.

<sup>2</sup>The first observation in a water Cherenkov detector of the corresponding  $\nu_\mu$ -induced reaction,  $\nu_\mu n \rightarrow \mu^- \pi^0 p$ , has been reported in [7].

<sup>3</sup>The cross sections of CC and NC reactions are quoted according to NEUGEN [8].

quasielastics because of less neutral-current background: two  $\pi^0$  mesons, and not just one, have to be produced in order to mimic the aforementioned 2- and 3-ring signatures. At neutrino energies of a few GeV in particular, the cross section of the NC reaction  $\nu N \rightarrow \nu\pi^0\pi^0N$  should be kinematically suppressed compared to  $\nu N \rightarrow \nu\pi^0N$ . This simple conjecture is supported by NEUGEN predictions<sup>4</sup>, see Fig. 1.

The values of oscillation parameters assumed in the simulation are  $\Delta m^2 = 0.003 \text{ eV}^2$ ,  $\sin^2 2\Theta_{23} = 1$ , and  $\sin^2 2\Theta_{13} = 0.1$  (that is, at the CHOOZ limit [9]). Matter effects are not accounted for, as here we only wish to compare the oscillation signals in the single-ring and multi-ring channels. Apart from enhancing the matter effect, increasing the baseline shifts the oscillation maximum to higher values of  $E_\nu$  where the cross sections of the reactions  $\nu_e n \rightarrow e^- \pi^0 p$  and  $\bar{\nu}_e p \rightarrow e^+ \pi^0 n$  are relatively big. Therefore, we select a baseline close to the maximum value for NuMI:  $L = 900$  km. The displacement from the axis of the NuMI medium-energy beam [1],  $R$ , is varied in the simulation. The  $E_\nu$  distribution of all  $\nu_\mu$ -induced CC events in the absence of oscillations, illustrated in Fig. 2 for the neutrino mode and  $R = 10$  km, peaks at  $E_\nu \simeq 2.6$  GeV. In the peak region, the intrinsic  $\nu_e$  component of the beam is some 0.3% of the  $\nu_\mu$  component (see Fig. 2). Running in the antineutrino mode will yield some 3 times less CC events for the same number of delivered protons.

Taking into account the experimental conditions of a water Cherenkov detector, actually simulated are the "quasi-inclusive" CC reactions  $\nu_e N \rightarrow e^- X$  and  $\nu_e N \rightarrow e^- \pi^0 X$ <sup>5</sup> and flavor-blind NC reactions  $\nu N \rightarrow \nu\pi^0 X$  and  $\nu N \rightarrow \nu\pi^0\pi^0 X$  in neutrino collisions with water. Here,  $X$  denotes a system of hadrons other than the  $\pi^0$ , in which the momenta of all charged particles are below the Cherenkov threshold in water. These reactions are analyzed in terms of visible energy  $E_{\text{vis}}$ , defined as a

---

<sup>4</sup>The uncertainties of these predictions for the cross sections of  $\nu_e n \rightarrow e^- \pi^0 p$  and  $\nu N \rightarrow \nu\pi^0\pi^0 N$  are hard to estimate, as the data are scarce for the former reaction and totally lacking—for the latter reaction.

<sup>5</sup>Respective antineutrino reactions are implicitly included.

sum over the energies of all detectable particles: the  $\pi^0$  mesons(s) and the charged lepton for CC reactions.

In a water Cherenkov detector, the two photons from  $\pi^0 \rightarrow \gamma\gamma$  may show up as a single  $e$ -like ring because of a small opening angle (this largely occurs at high  $\pi^0$  momenta), or because one of the photons from an "asymmetric"  $\pi^0$  decay is too soft to be detected [4]. The efficiency of  $\pi^0$  reconstruction as a function of its momentum will depend on the geometry and instrumentation of a Cherenkov detector; the estimates quoted below are based on the results for the 1-kiloton detector of K2K [10], as reported in [11]. The momenta of  $\pi^0$  mesons emitted in  $\nu_e N \rightarrow e^- \pi^0 X$  are plotted in Fig. 3, that also shows the distribution of reconstructed  $\pi^0$  mesons (lower histogram). We assume that at least one photon from  $\pi^0 \rightarrow \gamma\gamma$  is always detected, so that all 1-ring CC events arise from  $\nu_e N \rightarrow e^- X$  and all 1-ring NC events—from  $\nu N \rightarrow \nu \pi^0 X$  with unresolved photon showers. The probability for two photons to form a fake  $\pi^0$  candidate is neglected (in SuperK, the r.m.s. width of the  $\pi^0$  peak is only  $\sim 40$  MeV [11]). Depending on whether or not the  $\pi^0$  is reconstructible, a CC collision  $\nu_e N \rightarrow e^- \pi^0 X$  will produce 3 or 2 rings in the detector. NC events showing 3 (2) rings arise from failing to reconstruct one  $\pi^0$  (both  $\pi^0$ s) in the reaction  $\nu N \rightarrow \nu \pi^0 \pi^0 X$ .

The  $E_{\text{vis}}$  distributions<sup>6</sup> of events featuring 1, 2, and 3  $e$ -like rings are shown in Figs. 4–6 for incident neutrinos and different values of  $R$ . The three components of the  $E_{\text{vis}}$  distribution for either channel are: the  $\nu_\mu \rightarrow \nu_e$  signal (yellow area), the NC background (green area), and the intrinsic- $\nu_e$  background (red area). The  $E_{\text{vis}}$  interval for estimating the effect is selected so as to maximize the "Figure of Merit"  $S/\sqrt{B}$ , where  $S$  is the number of signal events and  $B$  is the total (NC plus intrinsic-CC) background. For either the  $\nu$  and  $\bar{\nu}$  settings of the beam, Table 1 compares the 1-ring and multi-ring samples in terms of total  $\nu_\mu \rightarrow \nu_e$  signals, num-

---

<sup>6</sup>Failing to reconstruct a  $\pi^0$  will but weakly affect the value of visible energy: in this case, either the two photons from  $\pi^0 \rightarrow \gamma\gamma$  have merged into a single shower sampled as a whole, or one of them is very soft.

bers of signal and background events in the selected  $E_{\text{vis}}$  windows, and statistical significance. Predictably, the ratio between the multi-ring and 1-ring signals decreases with increasing  $R$  (or off-axis angle). For incident neutrinos, the multi-ring signal is  $\sim 2$  times less than the 1-ring signal in absolute value, but has comparable significance due to less NC background. For incident antineutrinos, the multi-ring signal is substantially less significant than the 1-ring signal.

Beam, radius, signature	Total signal	$E_{\text{vis}}$ window	Signal in window	NC backgr.	Intr. CC backgr.	$S/\sqrt{B}$ (FoM)
$\nu$ , $R = 9$ km:						
1 ring	101.	2.2–3.2 GeV	61.	11.6	4.8	15.0
2 or 3 rings	51.	2.0–3.4 GeV	39.	7.5	3.6	11.6
$\nu$ , $R = 10$ km:						
1 ring	92.	2.0–3.0 GeV	60.	11.0	4.7	15.1
2 or 3 rings	44.	2.0–3.0 GeV	30.	4.2	2.4	11.5
$\nu$ , $R = 11$ km:						
1 ring	81.	1.8–2.8 GeV	57.	10.5	4.4	14.6
2 or 3 rings	37.	1.6–2.8 GeV	31.	5.6	2.5	10.9
$\bar{\nu}$ , $R = 9$ km:						
1 ring	80.	2.0–3.2 GeV	56.	5.0	4.9	17.9
2 or 3 rings	25.	2.0–3.2 GeV	17.	2.3	1.7	8.5
$\bar{\nu}$ , $R = 10$ km:						
1 ring	69.	1.8–3.0 GeV	53.	5.1	4.5	17.0
2 or 3 rings	20.	1.8–2.8 GeV	14.	1.9	1.2	7.8
$\bar{\nu}$ , $R = 11$ km:						
1 ring	59.	1.8–2.6 GeV	38.	3.2	2.8	15.3
2 or 3 rings	16.	1.6–2.8 GeV	12.	2.1	1.3	6.7

Table 1: The total  $\nu_\mu \rightarrow \nu_e$  ( $\bar{\nu}_\mu \rightarrow \bar{\nu}_e$ ) signal and the numbers of signal, NC background, and intrinsic-CC background events in the selected  $E_{\text{vis}}$  window for 1-ring and multi-ring signatures and for the  $\nu$  and  $\bar{\nu}$  settings of the beam. Also quoted is the "Figure of Merit"  $S/\sqrt{B}$ , where  $S$  is the number of signal events and  $B$  is the total (NC plus intrinsic-CC) background. The assumed exposure is 100 kton-years.

In a realistic Cherenkov detector, recoil protons often escape detection even for momenta above the Cherenkov threshold [12]. On average, recoil protons have higher momenta in  $\nu_e n \rightarrow e^- \pi^0 p$  than in  $\nu_e n \rightarrow e^- p$  due to a broader  $Q^2$  distribution, so that the multi-ring signal is expected to benefit most from keeping (some)

energetic protons. That lifting the upper cut on proton momentum effectively increases the ratio between the multi-ring and 1-ring signals is illustrated by Table 2, to be compared with Table 1.

Beam, radius, signature	Total signal	$E_{\text{vis}}$ window	Signal in window	NC backgr.	Intr. CC backgr.	$S/\sqrt{B}$ (FoM)
$\nu$ , $R = 9$ km:						
1 ring	133.	2.0–3.4 GeV	87.	24.9	8.7	14.9
2 or 3 rings	80.	2.0–3.2 GeV	49.	9.9	5.4	12.4
$\nu$ , $R = 10$ km:						
1 ring	119.	1.8–3.0 GeV	80.	22.0	7.2	14.9
2 or 3 rings	68.	1.6–3.0 GeV	51.	12.3	5.6	12.1
$\nu$ , $R = 11$ km:						
1 ring	105.	1.8–2.6 GeV	58.	12.3	4.6	14.1
2 or 3 rings	56.	1.6–2.6 GeV	37.	7.2	3.6	11.3

Table 2: The 1-ring and multi-ring signals of  $\nu_\mu \rightarrow \nu_e$  compared for incident neutrinos, no longer requiring that proton momenta be below the Cherenkov threshold in water.

As indicated in [3], fast PMT’s and good photocathode coverage may help discriminate between the electron- and  $\pi^0$ -induced showers by detecting the spatial separation between the conversion points of the two photons from  $\pi^0 \rightarrow \gamma\gamma$ . If shown to be realistic, this will equally apply to 1-ring and multi-ring signatures of  $\nu_\mu \rightarrow \nu_e$ . Yet another geometric handle may be possible for multi-ring topologies only, provided that spatial resolution of the detector is better than photon conversion length  $\lambda_c$ . An important advantage of having more than one ring is that constraining the axes of all rings to a common point in space will yield the position of the primary vertex. Within errors, this should coincide with the reconstructed vertex of a  $e^-$ -induced shower, whereas the vertex of an unresolved  $\pi^0$  shower will be displaced by  $\sim \lambda_c$  along the shower direction. The spatial resolution of SuperK has been estimated as 18 cm for the vertex of proton decay  $p \rightarrow e^+\pi^0$  whose signature is very similar to that of  $\nu_e n \rightarrow e^-\pi^0 p$ , and as 34 cm for the vertex of a single  $e$ -like ring [13]. We have  $\lambda_c \simeq 40$  cm for water, so that even a modest improvement in resolution over SuperK will allow to efficiently discriminate between CC and NC

multi-ring events and to measure the NC background (this of course needs to be checked by a detailed simulation of detector response).

To conclude, our preliminary results indicate that analyzing the reaction  $\nu_e n \rightarrow e^- \pi^0 p$  along with the quasielastic reaction  $\nu_e n \rightarrow e^- p$  may significantly enhance the sensitivity of a water Cherenkov detector to the "subleading" oscillation  $\nu_\mu \rightarrow \nu_e$  at neutrino energies  $\sim 2-3$  GeV. At the level of standard selections, the statistical significance of the multi-ring signal of  $\nu_\mu \rightarrow \nu_e$  is comparable to that of the 1-ring (quasielastic) signal. The antineutrino reaction  $\bar{\nu}_e p \rightarrow e^+ \pi^0 n$  is a less efficient probe of  $\bar{\nu}_\mu \rightarrow \bar{\nu}_e$  because its cross section is small. The NC background to  $\nu_e n \rightarrow e^- \pi^0 p$  can be suppressed by reconstructing the vertex of neutrino collision and analyzing spatial separation between the primary and secondary vertices.

## References

- [1] *Neutrino Oscillation Physics at Fermilab: the NuMI-MINOS Project*, Fermilab report NuMI-L-375, May 1998 (see [http://www.hep.anl.gov/ndk/hypertext/numi\\_notes.html](http://www.hep.anl.gov/ndk/hypertext/numi_notes.html)); V. Paolone, Nucl. Phys. Proc. Suppl. 100, 197 (2001).
- [2] Workshop on *New Initiatives for the NuMI Neutrino Beam*, Fermilab, May 2-4, 2002 (see [http://www-numi.fnal.gov/fnal\\_minos/new\\_initiatives](http://www-numi.fnal.gov/fnal_minos/new_initiatives)).
- [3] D. Ayres et al., *Letter of Intent to build an off-axis detector to study  $\nu_\mu \rightarrow \nu_e$  oscillations with the NuMI neutrino beam*, draft version 6.0, Fermilab, July 17, 2002 (see web site in [2]).
- [4] Y. Itow et al., *The JHF-Kamioka neutrino project*, arXiv:hep-ex/0106019.
- [5] See, for example, T. Kajita and Y. Totsuka, Rev. Mod. Phys. 73, 85 (2001).

- [6] D. Harris, *Far detector working group overview*, talk at the Workshop on New Initiatives for the NuMI Neutrino Beam, Fermilab, May 2002 (see web site in [2]).
- [7] S. Mine, *Study of  $\nu$  backgrounds to nucleon decay using K2K 1KT detector data*, talk at the NuInt01 Workshop, KEK, Dec. 2001 (see <http://neutrino.kek.jp/nuint01>).
- [8] H. Gallagher, *The NEUGEN neutrino event generator*, talk at the NuInt01 Workshop, KEK, Dec. 2001 (see web site in [7]); H. Gallagher and M. Goodman, *Neutrino Cross Sections*, Fermilab report NuMI-112, PDK-626, November 1995 (see web site in [1]).
- [9] M. Apollonio et al. (CHOOZ Coll.), Phys. Lett. B466, 415 (1999).
- [10] S.H. Ahn et al. (K2K Coll.), Phys. Lett. B511, 178 (2001); T. Ishii, *New results from K2K*, arXiv:hep-ex/0206033.
- [11] C. Mauger, *Neutral current  $\pi^0$  production in K2K and SuperK water Cherenkov detectors*, talk at the NuInt01 Workshop, KEK, Dec. 2001 (see web site in [7]).
- [12] R. Svoboda, private communication.
- [13] M. Shiozawa, in Proc. of RICH-98, Nucl. Instr. Meth. A433, 240 (1999).



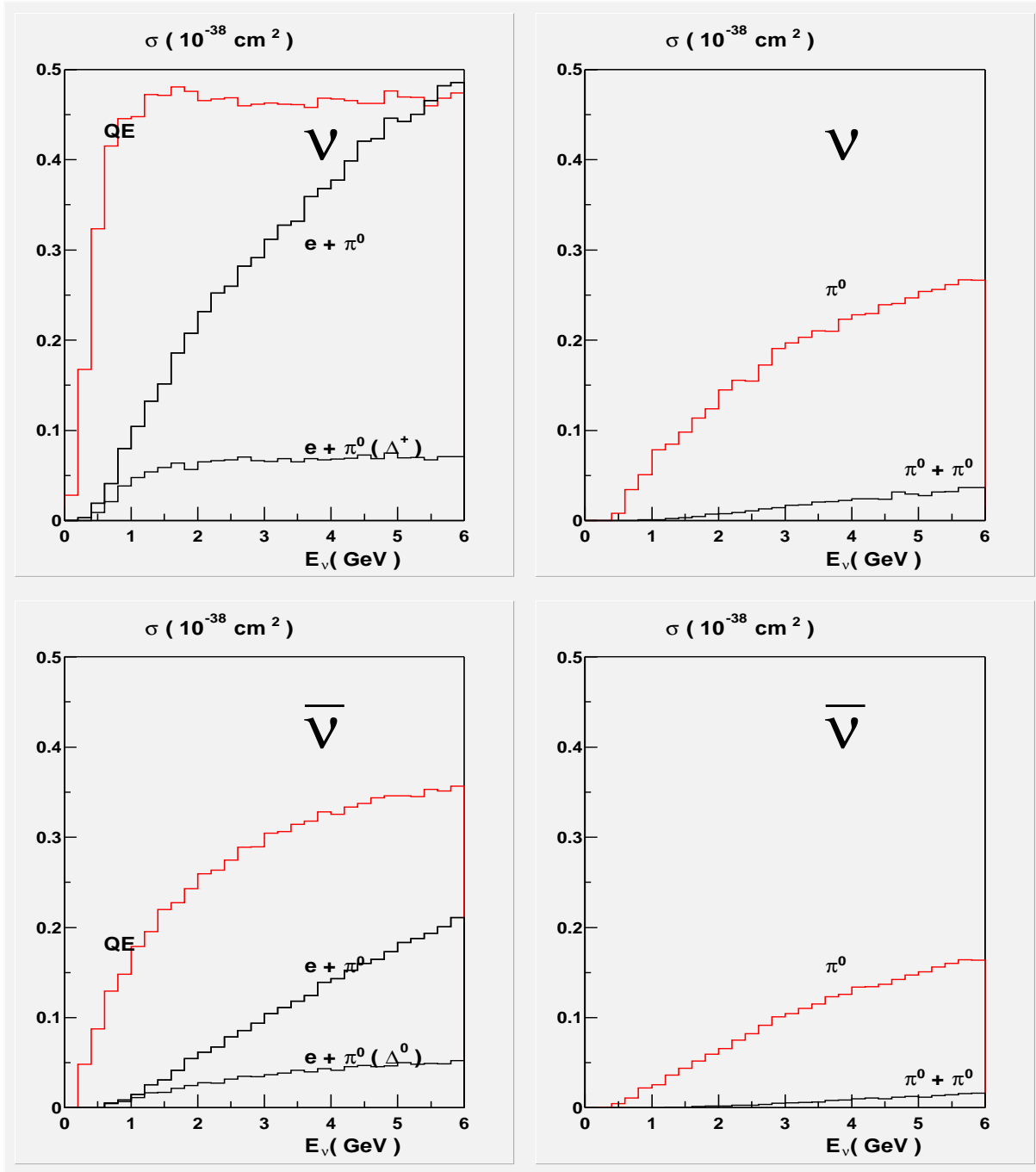


Figure 1: Cross sections per average nucleon in water of the reactions  $\nu_e n \rightarrow e^- p$  and  $\nu_e n \rightarrow e^- \pi^0 p$  (top left),  $\bar{\nu}_e p \rightarrow e^+ n$  and  $\bar{\nu}_e p \rightarrow e^+ \pi^0 n$  (bottom left),  $\nu N \rightarrow \nu \pi^0 N$  and  $\nu N \rightarrow \nu \pi^0 \pi^0 N$  (top right), and  $\bar{\nu} N \rightarrow \bar{\nu} \pi^0 N$  and  $\bar{\nu} N \rightarrow \bar{\nu} \pi^0 \pi^0 N$  (bottom right) as functions of neutrino energy. Also shown are the contributions of  $\Delta(1232)$  excitation to the  $\nu_e n \rightarrow e^- \pi^0 p$  and  $\bar{\nu}_e p \rightarrow e^+ \pi^0 n$  cross sections.

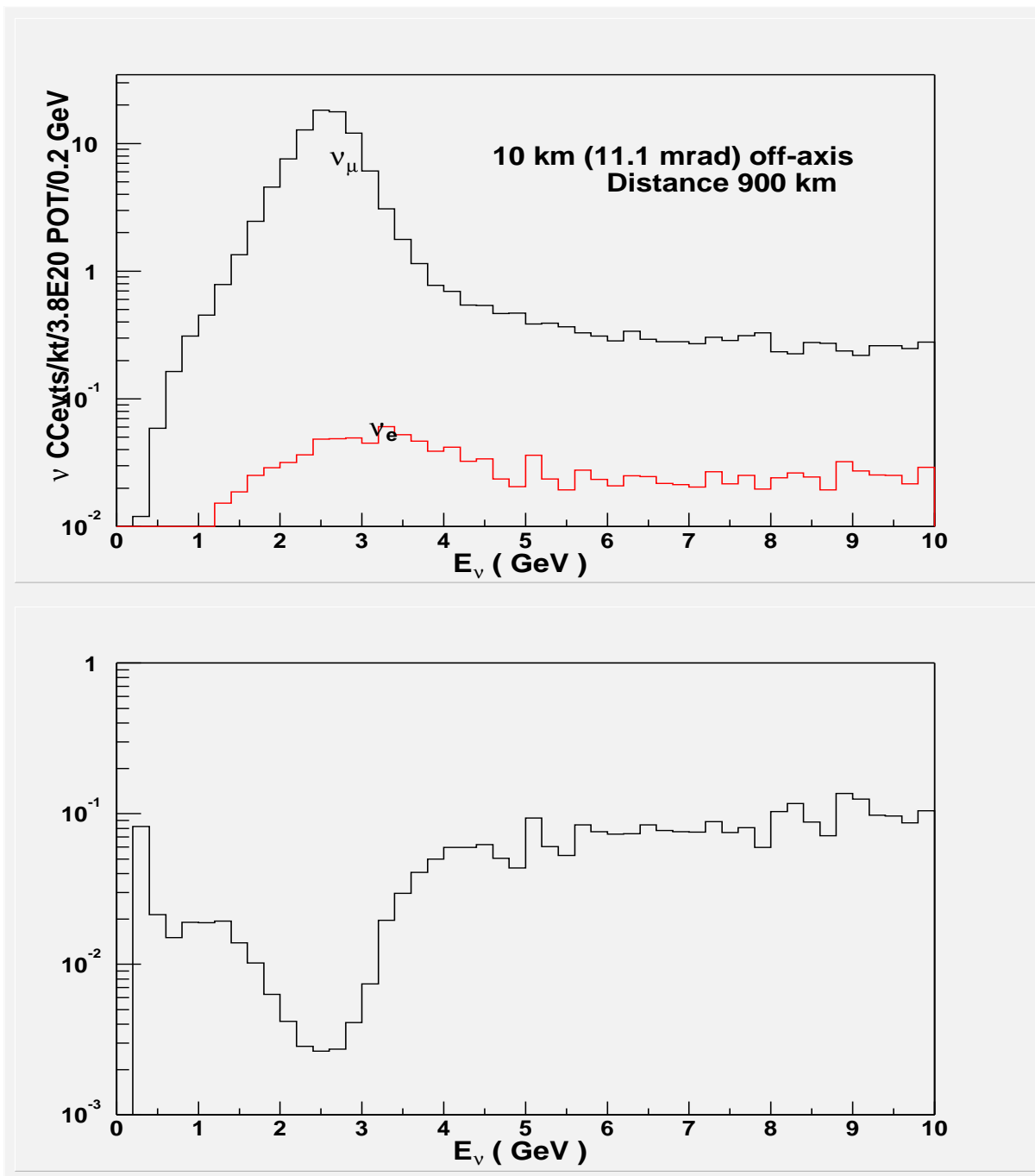


Figure 2: The oscillation-free  $E_\nu$  spectra of  $\nu_{e^-}$  and  $\nu_{\mu^-}$ -induced CC events (top panel) and their ratios (bottom panel) for an off-axis location in the NuMI medium-energy beam ( $L = 900$  km and  $R = 10$  km). The exposure is 100 kton-years.

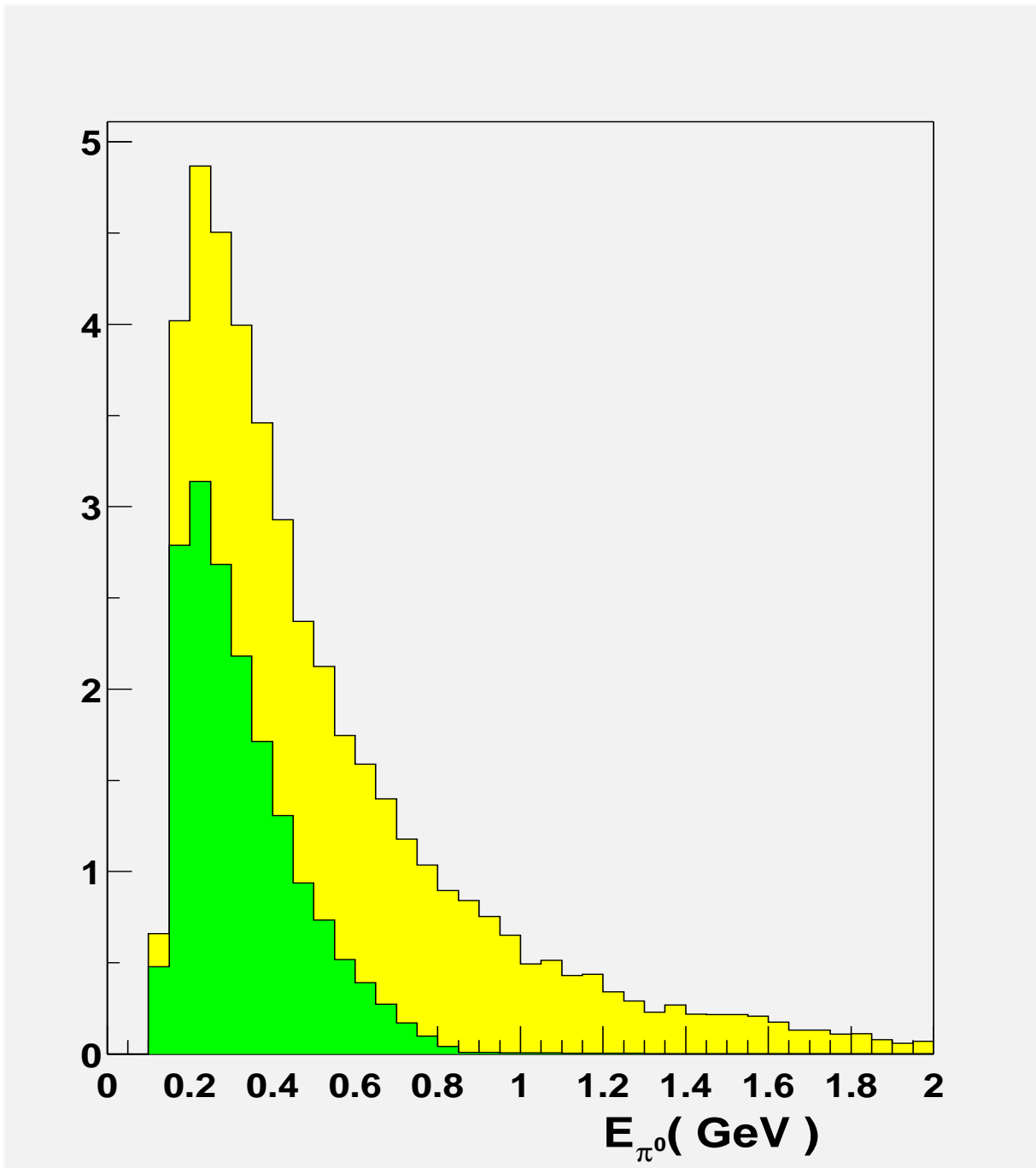


Figure 3: The momenta of  $\pi^0$  mesons emitted in the CC reaction  $\nu_e N \rightarrow e^- \pi^0 X$ . The lower histogram shows the contribution of reconstructed  $\pi^0$  mesons.

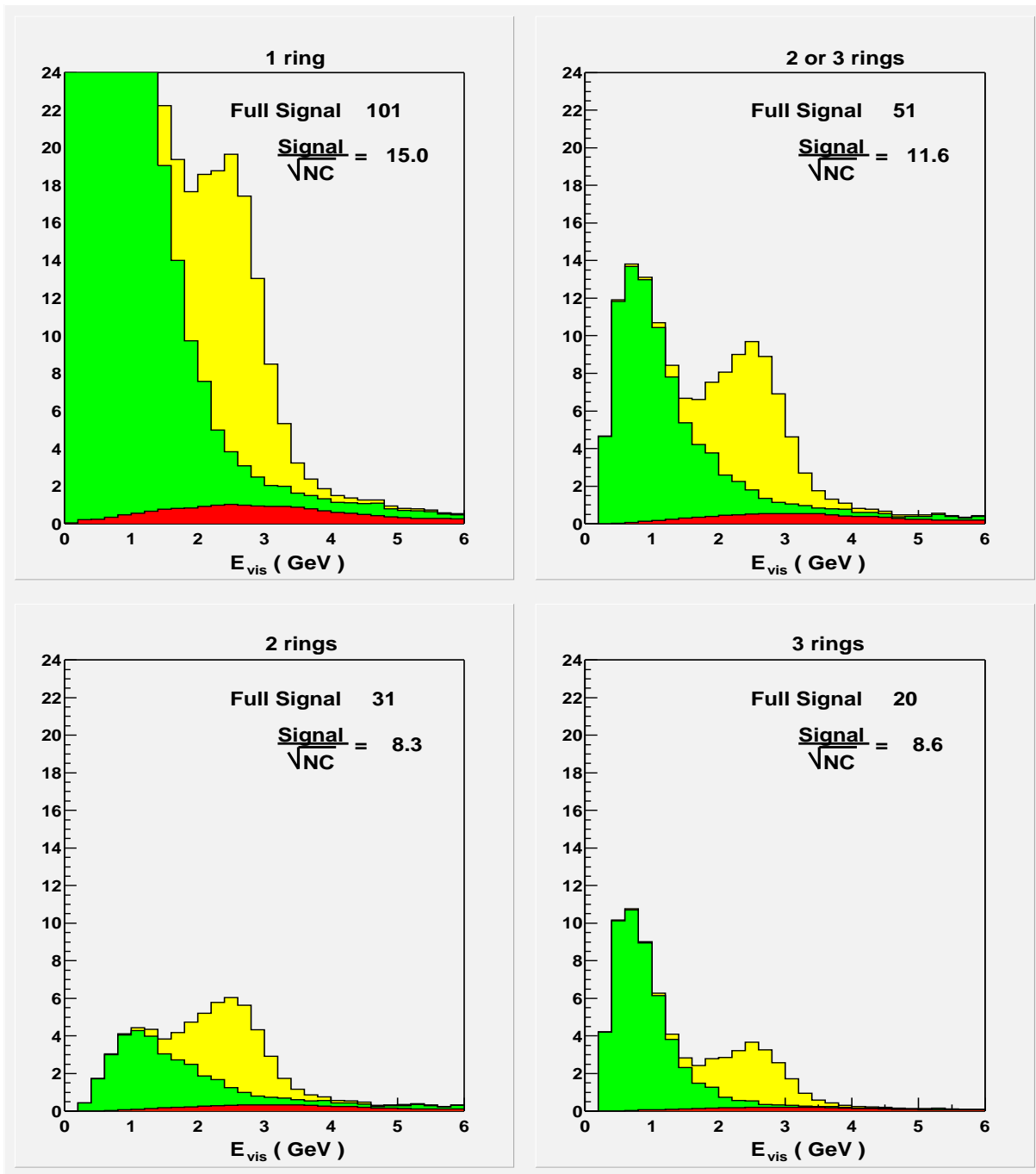


Figure 4:  $E_{vis}$  distributions of events featuring one  $e$ -like ring (top left), 2 or 3 rings (top right), 2 rings (bottom left), and 3 rings (bottom right). Here and in subsequent Figures, shown for either event category are the  $\nu_\mu \rightarrow \nu_e$  signal (yellow area), the NC background (green area), and the intrinsic CC background (red area). For incident neutrinos and  $R = 9$  km.

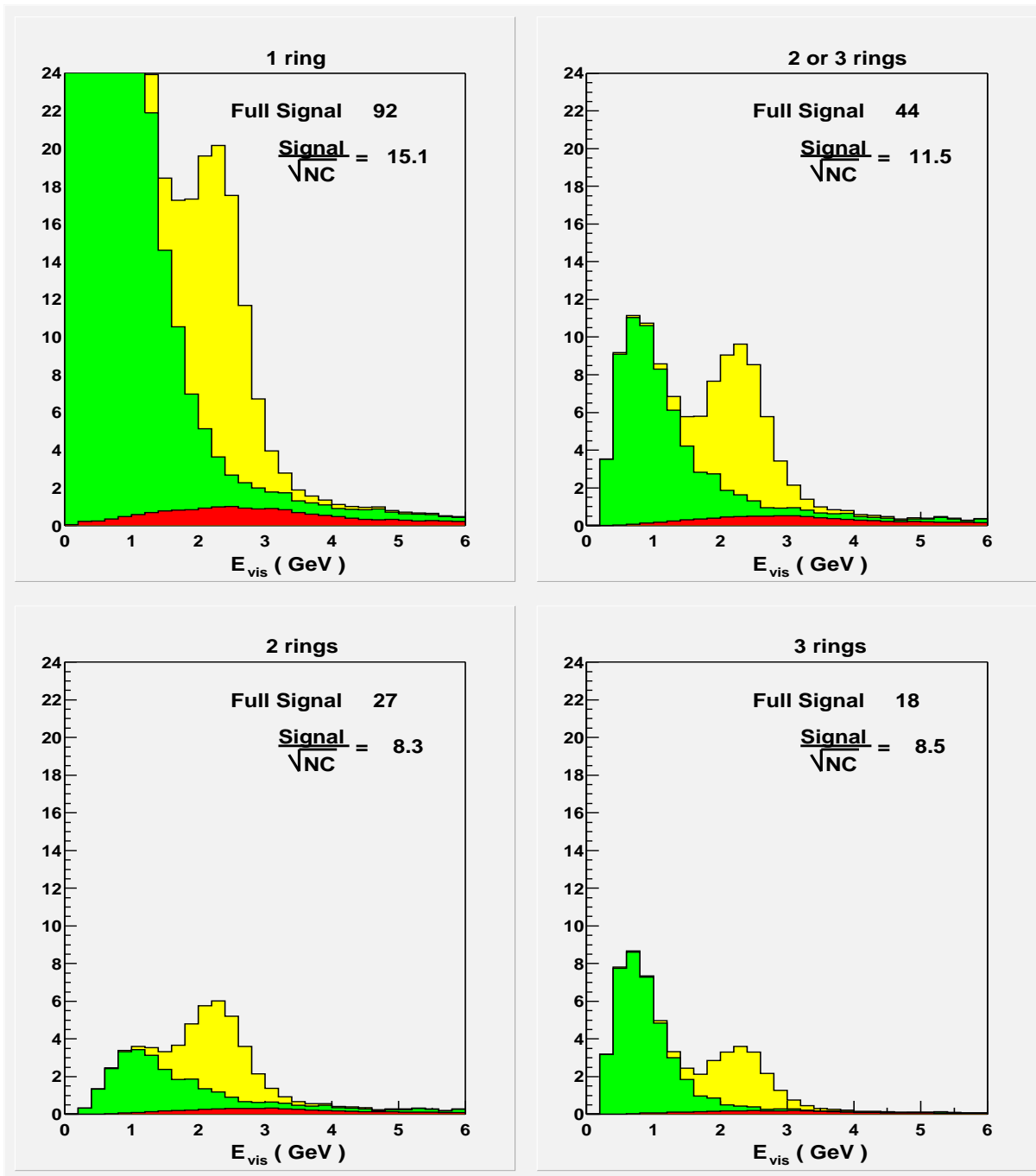


Figure 5:  $E_{\text{vis}}$  distributions of 1-ring and multi-ring events for incident neutrinos and  $R = 10$  km.

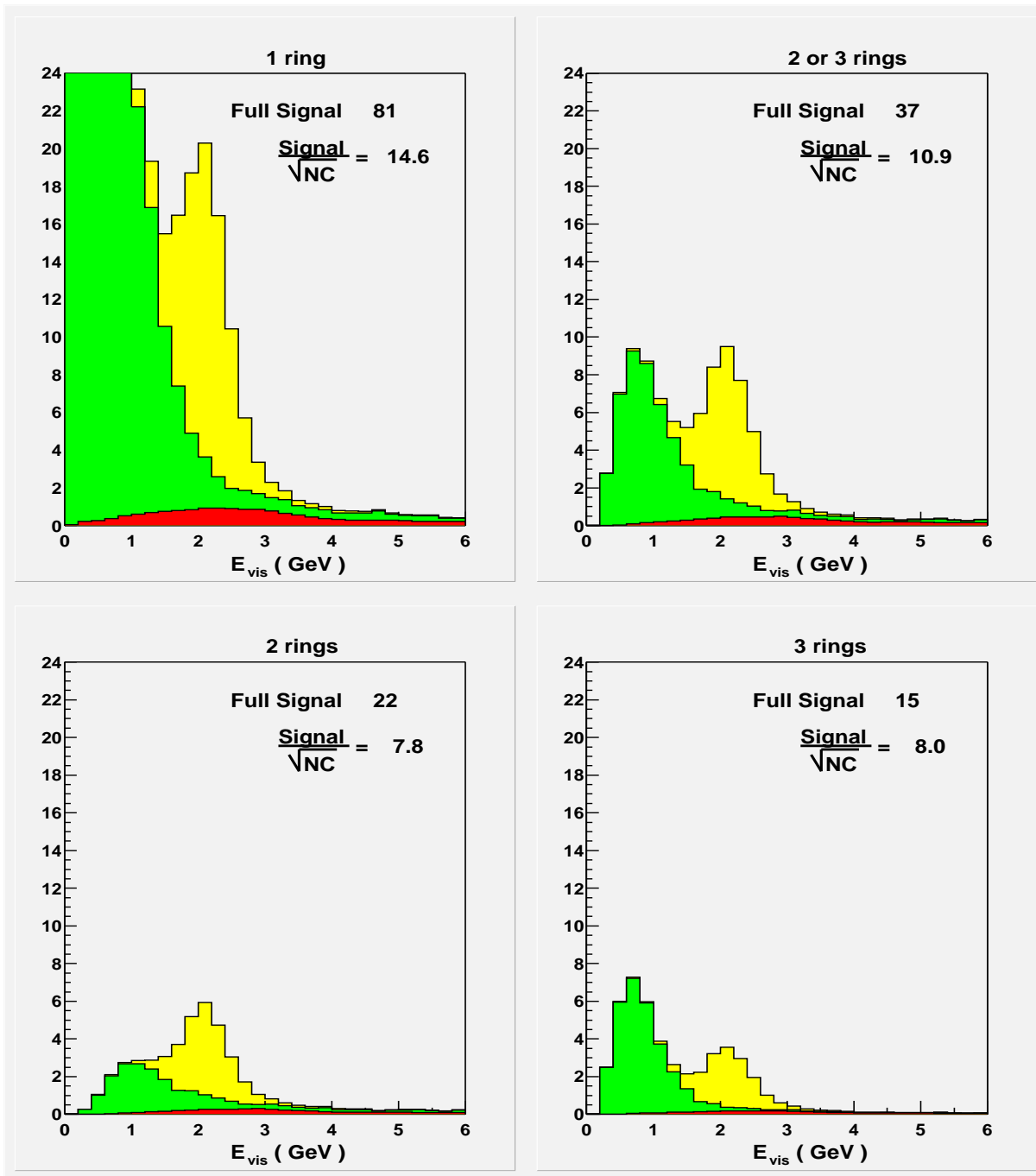


Figure 6:  $E_{\text{vis}}$  distributions of 1-ring and multi-ring events for incident neutrinos and  $R = 11$  km.